

## A Porous Crystalline Molecular Solid Explored by Hyperpolarized Xenon\*\*

Piero Sozzani,\* Angiolina Comotti, Roberto Simonutti, Thomas Meersmann, John W. Logan, and Alexander Pines

Porous materials are currently of great interest to several chemical fields, including catalysis, molecular confinement, and selective absorption.<sup>[1]</sup> Such materials have been obtained synthetically in several forms in addition to those found in nature.<sup>[2]</sup> Innovative principles developed in supramolecular chemistry<sup>[3]</sup> have been of help in obtaining self-assembled porous structures that, like zeolites, absorb atoms and molecules from the gas phase.<sup>[4]</sup> These materials are generally held together by directional forces that form extended frameworks of noncovalent interactions such as hydrogen bonds,  $\pi$ - $\pi$  interactions, or coordinate bonding. Recently, steric requirements have been used in designing new host molecules that pack efficiently with a number of guests.<sup>[5]</sup> Herein the shape and symmetry of the molecule is exploited to assemble a porous crystal where open nanochannels are stable in the absence of any guests. The  $D_3$  symmetry of tris(*o*-phenylenedioxy)cyclophosphazene<sup>[6]</sup> (TPP) allows a packing arrangement that does not satisfy the maximum filling principle.<sup>[7]</sup> Contrary to the reported examples of porous organic materials,<sup>[4]</sup> the molecular crystal of TPP does not contain stabilizing interactions except for weakly directional interactions.<sup>[8]</sup> Organic clathrates, such as perhydrotriphenylene and tri-*o*-thymotide, which are stabilized by van der Waals forces also contain sorbed molecules, but, when the guest molecules are removed the crystal structures generally collapse to a more stable crystal packing.<sup>[9]</sup> Even in some matrices where hydrogen bonding is present, such as urea, the removal of the guest molecules leads to the collapse of the crystal structure.<sup>[10]</sup> The novel polymorph of TPP absorbs guest atoms and molecules easily and when these are released the porous structure is retained (the accessible volume accounts for about 23 % of the total volume).

Continuous flow laser-polarized  $^{129}\text{Xe}$  NMR spectroscopy is applied for the first time to investigate the open-channel structure. An anisotropic signal from the xenon atoms inside the nanochannels is detected 200 ms after contact of the polarized gas with the sample. This observation is made

possible by the intense NMR response of the hyperpolarized xenon atoms<sup>[11]</sup> that are allowed to diffuse into the novel nanoporous modification of TPP. A unique case of one-dimensional diffusion of atoms into ideal, axially symmetric nanochannels is thus described.

The empty channellike structure could be obtained from the hexagonal TPP/benzene inclusion compound (IC) by mild evacuation of the volatile guest. The strategy to obtain the unusual polymorph of TPP was based on a careful study of the solid–solid transformation of the IC. The synthesis of the TPP molecule was performed as reported,<sup>[6]</sup> and the IC was prepared by crystallization from a solution in benzene. In the differential scanning calorimetric (DSC) analysis, the trace for the hexagonal phase exhibits a broad endotherm transition from 30–150 °C, an exotherm transition ( $|\Delta H| = 27.7 \text{ J g}^{-1}$ ) associated with the collapse to the monoclinic structure at 150 °C, and an endotherm transition (same enthalpy) at 225 °C followed by melting at 245 °C. The broad endotherm transition corresponds to the release of the volatile guests as confirmed by thermogravimetry analysis (TGA). Therefore only the thermal treatment at 75 °C (below the exotherm transition) and  $10^{-2}$  Torr generates the empty nanoporous polymorph (pseudo-hexagonal) and prevents the formation of the more stable structure (monoclinic). Thermogravimetric analysis indicates no release of volatile species until the melting point.

Figure 1a shows the structure of TPP and Figure 1b (top trace) the X-ray powder diffraction pattern of the pseudo

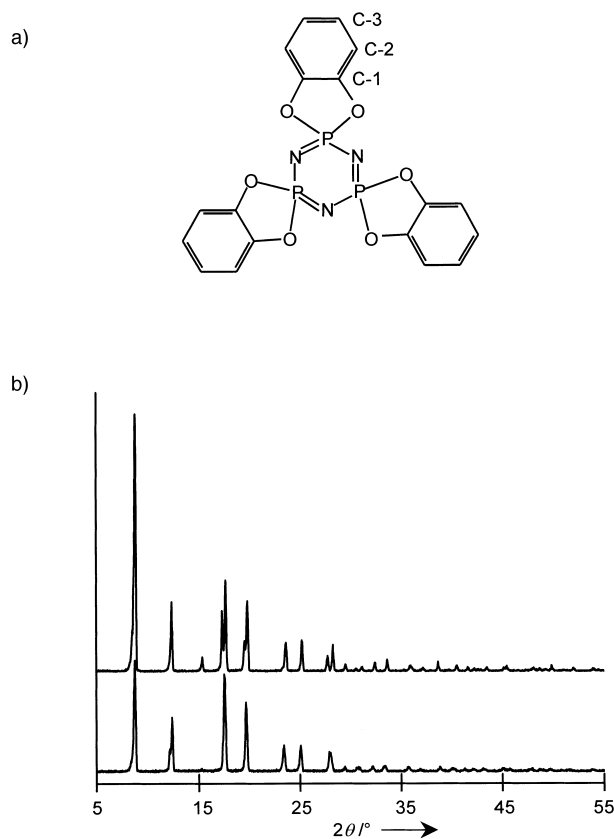


Figure 1. a) Molecular structure of TPP. b) X-ray powder diffraction pattern of the pseudo-hexagonal cell of the molecular zeolite TPP (top trace) and diffraction pattern of the hexagonal cell of the TPP/benzene IC (bottom trace).

[\*] Prof. P. Sozzani, Dr. A. Comotti, Dr. R. Simonutti  
Department of Materials Science  
Università di Milano—Bicocca  
via R. Cozzi 53, 20125 Milan (Italy)  
Fax: (+39)02-6448-5400  
E-mail: Piero.Sozzani@mater.unimib.it

Dr. T. Meersmann, J. W. Logan, Prof. A. Pines  
Department of Chemistry  
University of California  
and Materials Science Division  
Lawrence Berkeley National Laboratory, Berkeley, CA 94720 (USA)

[\*\*] We thank the Italian Ministry of Universities and Scientific Research (PRIN program) for financial support. The research with laser-polarized xenon was supported by the Director, Office of Energy Research, Office of Basic Energy Science, Materials Sciences Division of the U.S. Department of Energy. T.M. thanks the Alexander von Humboldt Foundation for a Feodor Lynen Fellowship.

hexagonal crystal cell (space group:  $P2_1/n$ ,  $a = 11.646(1)$ ,  $b = 10.2101(6)$ ,  $c = 11.5106(5)$ ,  $\beta = 119.939(5)$ ;  $Z = 2$ ,  $V = 1186 \text{ \AA}^3$ ,  $\rho_{\text{calcd}} = 1.233 \text{ g cm}^{-3}$ ).<sup>[12]</sup> The structure forms an empty channel surrounded by three TPP molecules at each level. For comparison, the X-ray diffraction pattern of the hexagonal packing of the TPP/benzene IC is shown in Figure 1 b (bottom trace, space group  $P6_3/m$ , cell parameters  $a = 11.6013(3)$ ,  $c = 10.0365(9)$ ).<sup>[13]</sup>

The multiplicity of the  $^{13}\text{C}$  and  $^{31}\text{P}$  MAS NMR signals (as detected at 75.5 and 121.5 MHz, respectively, on a Bruker MSL300 spectrometer) agrees with the symmetry of the pseudo-hexagonal crystal cell (Figure 2). The  $^{31}\text{P}$  MAS NMR spectrum (Figure 2 a) of the pseudo-hexagonal structure yields

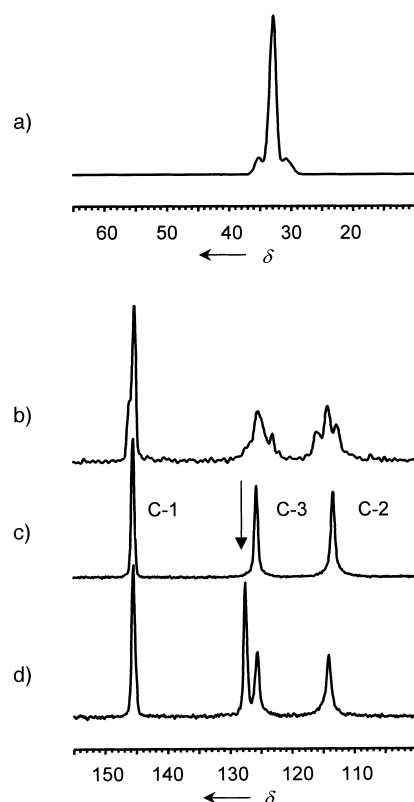


Figure 2. a)  $^{31}\text{P}$  MAS NMR spectrum of the pseudo-hexagonal cell. b)  $^{13}\text{C}$  Cross polarization (CP) MAS spectrum of the monoclinic cell (contact time of 8 ms). c)  $^{13}\text{C}$  MAS spectrum of the pseudo-hexagonal cell (recycle delay of 300 s). d)  $^{13}\text{C}$  MAS spectra of the TPP/benzene inclusion compound (recycle delay of 300 s).

one main peak at  $\delta = 32.9$ , which indicates that the phosphorus atoms are essentially equivalent in the unit cell.<sup>[14]</sup> The broad signals with low intensity derive from the  $^{31}\text{P}-^{14}\text{N}$  dipolar coupling which is not completely suppressed by magic angle spinning. The  $^{13}\text{C}$  MAS NMR spectrum (Figure 2 c) also reflects the high symmetry of the crystal cell since each type of aromatic carbon atom displays a single resonance line. The arrow in the spectrum indicates the frequency at which benzene molecules would resonate if they were still present. The  $^{13}\text{C}$  MAS NMR spectrum of the inclusion compound presents the same multiplicity as the pseudo-hexagonal structure, but with an additional peak at  $\delta = 127.3$  for the benzene guest molecules (Figure 2 d). The slight distortion of

the pseudo-hexagonal structure, relative to the hexagonal structure, is reflected in a shift of  $\delta = 1$  for the *ortho* carbon atom (C-2) resonance.<sup>[15]</sup> This shift is a result of the strong sensitivity of the chemical shift to the dihedral angle C(2)-C(1)-O-P, as already observed in tris(2,3-naphthalenedioxy)-cyclophosphazene.<sup>[16]</sup> For comparison, Figure 2 b shows the  $^{13}\text{C}$  CP MAS spectrum of the collapsed monoclinic structure devoid of channels: the presence of doublets and triplets for each type of aromatic carbon atom confirms the formation of the crystal cell with low symmetry.<sup>[17]</sup>

The above results demonstrate that the channel-like structure of the TPP crystal cell with benzene is maintained after removing the guest molecules at  $75^\circ\text{C}$ . It is reasonable to consider the guest-free cell as a zeolite-like structure: stable at room temperature and with channels accessible to volatile guests or even gases; xenon, in particular, is efficiently absorbed from the gas phase (Figures 3 a and b).<sup>[18]</sup>

The naturally occurring  $^{129}\text{Xe}$  isotope has a nucleus with  $I = \frac{1}{2}$  spin and  $^{129}\text{Xe}$  NMR spectroscopy is a tool for collecting information about the cavities in porous materials. The chemical shift of  $^{129}\text{Xe}$  is sensitive to the size of the cavities,

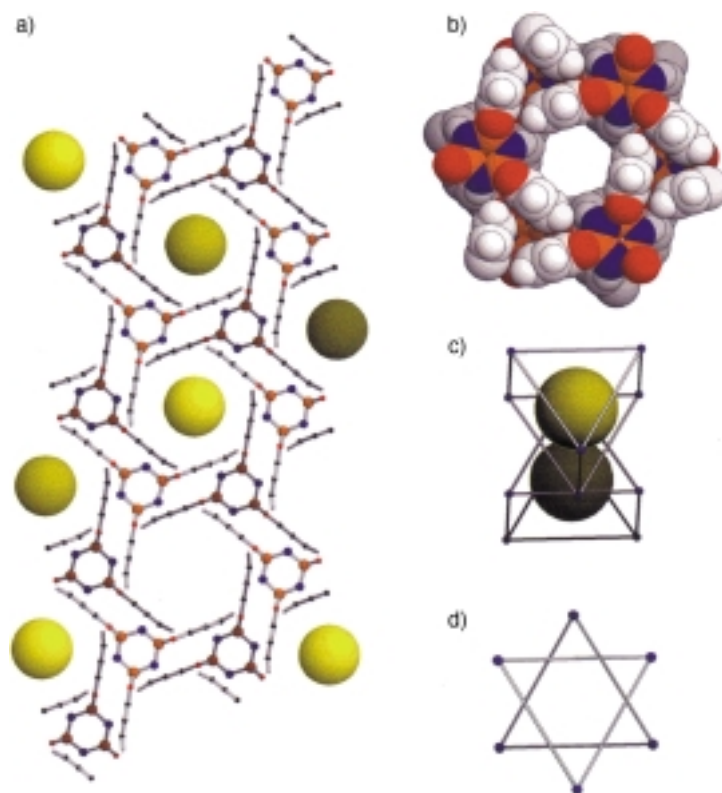


Figure 3. a) TPP channel-like structure viewed along the channel axis. Colors are as follows: gray: carbon, red: oxygen, blue: phosphorus, orange: nitrogen, white: hydrogen, yellow: xenon. Broken bonds indicate an extension of the structure. The darkening of the Xe yellow color indicates the depth of the atoms along the channels. The TPP molecule packing results in the formation of cavities which are partially occupied by Xe atoms at low loading. b) The channel-like structure of TPP based on the van der Waals radii viewed along the channel axis. The channel walls are formed by aromatic units parallel to the channel axis; the nitrogen atoms face the channel. c) The geometry of the cavities as viewed by perspective. d) The geometry of the cavities as viewed along the channel axis. The cavity shape corresponds to a prism with a triangular base. The prisms are stacked along the channel axis rotated by  $60^\circ$  with respect to the others, thus producing a hexagonal shape.

and the anisotropic profile of the confined gas atoms gives an insight into the geometry of the space explored.<sup>[19]</sup> In this particular case, the TPP nanochannels were explored by hyperpolarized xenon NMR spectroscopy.<sup>[11]</sup> This highly innovative technique gives rise to an intense NMR signal for the diffusing atoms in just one scan. Moreover, continuous-flow laser-polarized  $^{129}\text{Xe}$  NMR spectroscopy provides a means of demonstrating the easy accessibility of the nanochannels to gas atoms, which allows an investigation of the first stages of xenon diffusion into the nanochannels.<sup>[20]</sup> The recycle time between the NMR reading pulses determines the time scale for entry of xenon into the channels. It has been possible to obtain observable  $^{129}\text{Xe}$  NMR spectra of continuously replaced laser-polarized xenon inside the TPP channels with recycle times as short as 200 ms. This is a noteworthy result that indicates the rapid diffusion of xenon into the nanochannels.

Figure 4 shows the  $^{129}\text{Xe}$  NMR spectra of laser-polarized xenon following diffusion into porous crystalline material (as detected at 138.3 MHz on a Chemagnetics 500 spectrometer) for several xenon/helium gas mixtures. The high sensitivity of the technique allows the detection of xenon concentrations as low as 1% diluted in helium. The laser-polarized xenon gives rise to anisotropic signals centered around  $\delta = 110$ , with the line shape depending on the xenon partial pressure. At a

concentration of 1% xenon the line shape indicates an axially symmetric chemical shift anisotropy (CSA) with positive anisotropy.<sup>[21]</sup> Increasing the xenon partial pressure leads to an inversion of the sign of the anisotropy. The anisotropy parameter  $\Delta\delta$ , obtained from the numerical fitting of the CSA powder pattern,<sup>[22]</sup> ranges between  $\delta = +22.1$  at 1% xenon and  $\delta = -12.2$  at 100%. Although the inversion of the anisotropy was previously observed in nonaxially symmetric systems,<sup>[23]</sup> the present experiments under axial symmetry of the xenon CSA have shown the collapse of the line shape to a narrow isotropic signal at a xenon concentration of 30%. The CSA powder patterns present small values for the asymmetry parameters  $\eta$  of 0.12–0.14.<sup>[21, 22]</sup>

In order to explain these results let us consider the TPP channels composed of stacked prisms with triangular bases twisted by  $60^\circ$  (Figure 3c), with the TPP aromatic rings constituting the vertical faces. Hexagonal restriction forms connections of about  $5 \text{ \AA}$  between the prisms (Figure 3d). Within the limits of rapid diffusion the space explored by the xenon atoms appears, on average, to be a cylinder with a diameter slightly larger than the  $4.4 \text{ \AA}$  diameter of the xenon atom.<sup>[12]</sup> The  $\pi$  electrons of the TPP aromatic units face the interior of the channel and are in close proximity to the essentially one-dimensional, fast-diffusing guest atoms. Thus, the NMR spectra suggest that the axial symmetry of the channel is imposed on the xenon atoms. Two sources for the average shape of the xenon electron cloud are the xenon–xenon interactions and the interaction of the xenon atoms with the nanochannel wall.<sup>[24]</sup> At low xenon concentrations there are fewer xenon–xenon collisions, and the xenon–wall interaction dominates the density distribution of the electron cloud of the xenon atom. At high xenon concentrations the interaction between xenon atoms is enhanced relative to the xenon–wall interaction. The change from an oblate to a prolate electronic symmetry of the electron shell is reflected in the sign change of the chemical shift anisotropy.

The unprecedented and clear evidence of a “null” (pseudoisotropic) point at a Xe concentration of 30% is consistent with the qualitative features of the model: at this point the two competing interactions (xenon–wall and xenon–xenon) are balanced, and the shape of the xenon atoms are dynamically averaged to an effectively spherical, isotropic symmetry.

The results of our experiments support the model of zeolite-like open channels that readily absorb gases that run along a one-dimensional file.<sup>[25]</sup> The structure very closely resembles that of zeolite materials containing channels of  $5\text{--}8 \text{ \AA}$ .<sup>[23]</sup> In most known cases the shape of the zeolite channels deviates from a cylindrical geometry and may contain, at different levels, elliptical cross-sections.<sup>[26]</sup> The uniqueness of the system is that the nanopore shape is close to an ideal cylinder. The small values found for the asymmetry parameter  $\eta$  suggest only a slight distortion from the hexagonal symmetry, and this is consistent with the pseudohexagonal cell determined from the X-ray diffraction data.

In conclusion, this work describes a crystalline modification held together by weakly directional forces containing open channels. The crystal phase provides an unusual  $\pi$ -electron rich environment for the one-dimensional diffusion of atoms, on the other hand xenon anisotropic signals show the

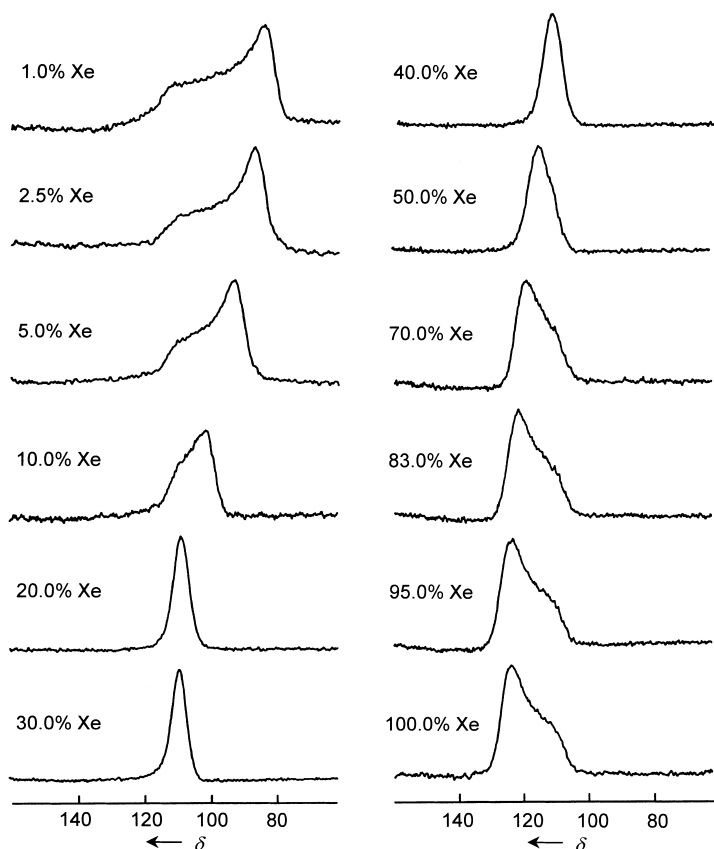


Figure 4. Continuous-flow laser-polarized  $^{129}\text{Xe}$  NMR<sup>[20]</sup> spectra of Xe/He mixtures flowing in the TPP pseudohexagonal phase at atmospheric pressure and room temperature. The time for diffusion of the optically polarized xenon into the TPP channels was set by the recycle delay to 200 ms. The components of the CSA tensors ( $\delta_{11}$ ,  $\delta_{22}$ , and  $\delta_{33}$ ) calculated by a numerical fitting procedure are reported in ref. [22].

squeezing of the atoms into the crystal nanochannels. In this example we were able to detect such an anisotropic xenon signal 200 ms after the gas diffusion into the aromatic nanochannel. The anisotropy of a gas diffusing into a crystal has been rarely observed, and never by advanced NMR techniques. We believe, the results are relevant to the field of supramolecular engineering, atomic confinement, and the developing of models for single-file diffusion.

Received: March 20, 2000 [Z14869]

- [1] a) G. Férey, A. K. Cheetham, *Science* **1999**, *283*, 1125–1126; b) C. W. Jones, K. Tsuji, M. E. Davis, *Nature* **1998**, *393*, 52–54; c) C. N. R. Rao, *J. Mater. Chem.* **1999**, *9*, 1–14; d) G. A. Ozin, C. T. Kresge, S. M. Yang, N. Coombs, I. Sokolov, *Adv. Mater.* **1999**, *11*, 1427–1431.
- [2] a) R. M. Barrer, *Zeolites and Clay Minerals as Sorbent and Molecular Sieves*, Academic Press, London, **1978**; b) D. W. Brek, *Zeolite Molecular Sieves*, Wiley, New York, **1984**; c) C. T. Kresge, M. E. Leonowicz, W. J. Roth, J. C. Vartuli, J. S. Beck, *Nature* **1992**, *359*, 710–712; d) T. E. Gier, X. Bu, P. Feng, G. D. Stucky, *Nature* **1998**, *395*, 154–157.
- [3] J.-M. Lehn, *Supramolecular Chemistry: Concepts and Perspective*, VCH, Weinheim, **1995**.
- [4] a) O. M. Yaghi, G. Li, H. Li, *Nature* **1995**, *378*, 703–706; b) P. Brunet, M. Simard, J. D. Wuest, *J. Am. Chem. Soc.* **1997**, *119*, 2737–2738; c) B. T. Ibragimov, S. A. Talipov, T. F. Aripov, *J. Inclusion Phenom. Mol. Recognit. Chem.* **1994**, *17*, 317–324; d) R. Bishop, D. C. Craig, M. L. Scudder, A. P. Marchand, Z. Liu, *J. Chem. Soc. Perkin Trans 2* **1995**, *2*, 1295–1300; e) K. Endo, T. Sawaki, M. Koyanagi, K. Kobayashi, H. Masuda, Y. Aoyama, *J. Am. Chem. Soc.* **1995**, *117*, 8341–8352; f) G. B. Gardner, Y.-H. Kiang, S. Lee, A. Asgaonkar, D. Venkataraman, *J. Am. Chem. Soc.* **1996**, *118*, 6946–6953.
- [5] K. Kobayashi, T. Shirasaka, A. Sato, E. Horn, N. Furukawa, *Angew. Chem.* **1999**, *111*, 3692–3694; *Angew. Chem. Int. Ed.* **1999**, *38*, 3483–3486.
- [6] H. R. Allcock, L. A. Siegel, *J. Am. Chem. Soc.* **1964**, *86*, 5140–5144.
- [7] C. P. Brock, J. D. Dunitz, *Chem. Mater.* **1994**, *6*, 1118–1127.
- [8] Weakly directional interactions are defined as in: G. R. Desiraju in *Comprehensive Supramolecular Chemistry, Vol. 6* (Eds.: J. L. Atwood, J. E. Davies, D. D. MacNicol, F. Vögtle), Pergamon, Oxford, **1996**, pp. 1–22.
- [9] a) M. Farina, G. Di Silvestro, P. Sozzani in *Comprehensive Supramolecular Chemistry, Vol. 6* (Eds.: J. L. Atwood, J. E. Davies, D. D. MacNicol, F. Vögtle), Pergamon, Oxford, **1996**, pp. 371–398; b) R. Arad-Yellin, B. S. Green, M. Knossow, G. Tsoucaris in *Inclusion Compounds, Vol. 6* (Eds.: J. L. Atwood, J. E. D. Davies, D. D. MacNicol), Academic Press, New York, **1988**, pp. 278–284.
- [10] M. D. Hollingsworth, K. D. Harris in *Comprehensive Supramolecular Chemistry, Vol. 6* (Eds.: J. L. Atwood, J. E. Davies, D. D. MacNicol, F. Vögtle), Pergamon, Oxford, **1996**, pp. 177–237.
- [11] a) D. Raftery, H. Long, T. Meersmann, P. J. Grandinetti, L. Reven, A. Pines, *Phys. Rev. Lett.* **1991**, *66*, 584–587; b) D. Raftery, E. MacNamara, G. Fisher, C. V. Rice, J. J. Smith, *J. Am. Chem. Soc.* **1997**, *119*, 8746–8747; c) M. Haake, A. Pines, J. A. Reimer, R. Seydoux, *J. Am. Chem. Soc.* **1997**, *119*, 11711–11712.
- [12] The X-ray powder diffraction pattern associated with the TPP/H<sub>2</sub>O inclusion compound is absent. H. R. Allcock, M. L. Levin, R. R. Whittle, *Inorg. Chem.* **1986**, *25*, 41–47.
- [13] H. R. Allcock, R. W. Allen, E. C. Bissell, L. A. Smeltz, M. Teeter, *J. Am. Chem. Soc.* **1976**, *98*, 5120–5125.
- [14] The collapsed monoclinic structure shows three phosphorus peaks, according to the lower symmetry. A. Comotti, R. Simonutti, S. Stramare, P. Sozzani, *Nanotechnology* **1999**, *10*, 70–76.
- [15] The chemical shifts of the pseudo-hexagonal cell are  $\delta = 145.3$ , 125.5, and 113.1 for the C-1, C-3, and C-2 carbon atoms, respectively. The hexagonal cell shows the following chemical shifts:  $\delta = 145.3$ , 125.5, and 114.1 for the C-1, C-3, and C-2 carbon atoms, respectively.
- [16] a) A. Comotti, M. C. Gallazzi, R. Simonutti, P. Sozzani, *Chem. Mater.* **1998**, *10*, 3589–3596; b) P. Sozzani, A. Comotti, R. Simonutti in *Crystal Engineering: From Molecules and Crystals to Materials* (Eds.: D. Braga, F. Grepioni, A. G. Orpen), NATO Sciences Series, Kluwer Academic Publishers, The Netherlands, **1999**, pp. 443–458.
- [17] The collapsed monoclinic structure (space group:  $P2_1/n$ ) presents the following cell parameters:  $a = 25.297(2)$ ,  $b = 5.9368(4)$ ,  $c = 26.125(2)$ ,  $\beta = 96.211(7)$ ,  $V = 3900.5 \text{ \AA}^3$ ,  $\rho_{\text{calcd}} = 1.500 \text{ g cm}^{-3}$ .
- [18] Empty nanoporous TPP (270.5 mg) reduced the xenon pressure in a volume of 22.1 cm<sup>3</sup> from 310 to 225 torr during the course of 5 min (0.17 mol Xe per mol of TPP). Microbalance measurements made it possible to follow xenon sorption with time at constant pressure: the sorption of 0.52 mol of Xe per mol of matrix is reached in a few hours at 280 Torr by the pseudo-hexagonal form. No gas sorption is exhibited by the monoclinic TPP form under the same conditions. As an example of volatile molecules being sorbed from the vapour phase, the benzene pressure was reduced from 15.6 to 4.5 Torr in 15 min when benzene vapours were sealed at 22 °C in a glass chamber of 22.6 cm<sup>3</sup> in the presence of 53 mg of TPP. No reduction of pressure within  $\pm 1$  Torr was observed in the presence of the monoclinic phase.
- [19] a) T. Ito, J. Fraissard, *J. Chem. Phys.* **1982**, *76*, 5225; b) J. A. Ripmeester, *J. Am. Chem. Soc.* **1982**, *104*, 289–290.
- [20] a) A. Bifone, T. Pietrass, J. Kritzenberger, A. Pines, B. F. Chmelka, *Phys. Rev. Lett.* **1995**, *74*, 3277–3280; b) M. S. Albert, G. D. Cates, B. Driehuys, W. Happer, B. Saam, C. S. Springer, Jr., A. Wishnia, *Nature* **1994**, *370*, 199–201; c) G. Navon, T. Q. Song, T. Room, S. Appelt, R. E. Taylor, A. Pines, *Science* **1996**, *271*, 1848–1851.
- [21] Definitions used for the CSA tensor elements:  $\delta_{\text{iso}} = (\delta_{11} + \delta_{22} + \delta_{33})/3$ ;  $|\delta_{33} - \delta_{\text{iso}}| > |\delta_{22} - \delta_{\text{iso}}| > |\delta_{11} - \delta_{\text{iso}}|$ ;  $\Delta\delta = \delta_{33} - \delta_{\text{iso}}$ ;  $\eta = |\delta_{22} - \delta_{11}| / |\delta_{33} - \delta_{\text{iso}}|$ .
- [22] The CSA tensor elements ( $\delta_{11}$ ,  $\delta_{22}$ ,  $\delta_{33}$ ) obtained by numerical fitting are the following:  $\delta = 83.3$ , 80.2, and 114.9 for 1.0% xenon; 85.1, 82.7, and 113.6 for 2.5% xenon; 91.2, 89.4, and 113.5 for 5.0% xenon; 99.6, 98.5, and 112.3 for 10% xenon; 115.4, 116.0, and 107.8 for 50.0% xenon; 119.2, 120.5, and 105.6 for 70% xenon; 121.6, 123.1, and 106.0 for 83.0% xenon; 123.6, 125.2, and 106.2 for 95.0% xenon; 124.3, 126.0, and 106.8 for 100.0% xenon. At xenon concentrations of 20%, 30%, and 40% the spectra present a lorentzian peak with the following values:  $\delta = 107.9$  and line-width 332 Hz for 20% xenon;  $\delta = 109.2$  and line-width 317 Hz for 30% xenon;  $\delta = 111.5$  and line-width 387 Hz for 40% xenon.
- [23] a) M. A. Springuel-Huet, J. Fraissard, *Chem. Phys. Lett.* **1989**, *154*, 299–302; b) J. A. Ripmeester, C. I. Ratcliffe, *J. Phys. Chem.* **1995**, *99*, 619–622.
- [24] In the presence of xenon no structural changes of the matrix could be observed by X-ray diffraction analysis.
- [25] V. Kukla, J. Kornatowski, D. Demuth, I. Girnus, H. Pfeifer, L. V. C. Rees, S. Schunk, K. K. Unger, J. Kärger, *Science* **1996**, *272*, 702–704.
- [26] M. W. Anderson, J. Klinowski, *Nature* **1989**, *339*, 200–203.